

Table S1. List of sequences used in this study.

Species	Identifier	Database
Angiosperm NRPE1 homologs		
<i>Amborella trichopoda</i>	evm_27.model.AmTr_v1.0_scaffold00131.41	Amborella Genome
<i>Arabidopsis thaliana</i>	AT2G40030	TAIR
<i>Aquilegia coerulea</i>	Acoerulea.22047564 Acoerulea.22025488	Phytozome 10
<i>Citrus clementina</i>	Cclementina.20791338	Phytozome 10
<i>Citrus sinensis</i>	Csinensis.18120100	Phytozome 10
<i>Cucumis sativus</i>	Csativus.16978203	Phytozome 10
<i>Eucalyptus grandis</i>	Egrandis.23599136	Phytozome 10
<i>Fragaria vesca</i>	Fvesca.27249047	Phytozome 10
<i>Glycine max</i>	Gmax.30498456 Gmax.30505760	Phytozome 10
<i>Gossypium raimondii</i>	Graimondii.26760711	Phytozome 10
<i>Linum usitatissimum</i>	Lusitatissimum.23162059	Phytozome 10
<i>Medicago truncatula</i>	Mtruncatula.31075688	Phytozome 10
<i>Mimulus guttatus</i>	Mguttatus.28945928	Phytozome 10
<i>Oryza sativa</i>	LOC_Os01g73430 LOC_Os02g05880	Phytozome 10
<i>Panicum virgatum</i>	Pvirgatum.30305942 Pvirgatum.30252426	Phytozome 10
<i>Phaseolus vulgaris</i>	Pvulgaris.27152868	Phytozome 10
<i>Prunus persica</i>	Ppersica.17669039	Phytozome 10
<i>Populus trichocarpa</i>	Ptrichocarpa.27003419 Ptrichocarpa.26998728	Phytozome 10
<i>Salix purpurea</i>	Spurpurea.31444571	Phytozome 10
<i>Setaria italica</i>	Sitalica.19697436 Sitalica.19688672	Phytozome 10
<i>Solanum lycopersicum</i>	Slycopersicum.27300428	Phytozome 10
<i>Sorghum bicolor</i>	Sbicolor.28384871	Phytozome 10
<i>Theobroma cacao</i>	Tcacao.27443915	Phytozome 10
<i>Vitis vinifera</i>	Vvinifera.17824747	Phytozome 10
Oryza and related NRPE1a		
<i>Brachypodium distachyon</i>	Bradi4g45065	Phytozome
<i>Leersia perrieri</i>	LPERR02G03610	EnsemblPlants
<i>Oryza barthii</i>	OBART02G04100	EnsemblPlants

<i>Oryza brachyantha</i>	OB02G13460	EnsemblPlants
<i>Oryza glaberrima</i>	ORGLA02G0038200	EnsemblPlants
<i>Oryza glumaepatula</i>	OGLUM02G03900	EnsemblPlants
<i>Oryza longistaminata</i>	OLONG_014977	EnsemblPlants
<i>Oryza meridionalis</i>	OMERIO204920	EnsemblPlants
<i>Oryza nivara</i>	ONIV02G04030	EnsemblPlants
<i>Oryza punctata</i>	OPUNC02G03300	EnsemblPlants
<i>Oryza rufipogon</i>	ORUFI02G04170	EnsemblPlants
<i>Oryza sativa ssp japonica</i>	LOC_Os02g05880	Phytozome
<i>Oryza sativa ssp indica</i>	BGIOGA007122	EnsemblPlants
<i>Triticum aestivum</i>	genomic region near Traes_6AS_B5ED3BA5B	Phytozome

Brassicaceae and related NRPE1

<i>Aethionema arabicum</i>	n.a. ¹	CoGe
<i>Arabidopsis arenosa</i>	n.a. ²	SRA PRJNA196706 ³
<i>Arabidopsis halleri</i>	Araha.54531s0001	Phytozome 10
<i>Arabidopsis lyrata</i>	483042	Phytozome 10
<i>Bochera strica</i>	Bostr.23794s0061	Phytozome 10
<i>Brassica oleraceae</i>	Bo3g034650	EnsemblPlants
<i>Brassica rapa</i>	Bra000162	EnsemblPlants
<i>Camelina sativa</i>	n.a. ¹	CoGe
<i>Capsella grandiflora</i>	Cagra.2495s0018	CoGe
<i>Capsella rubella</i>	Carubv10022497m	Phytozome 10
<i>Eutrema salsugineum</i>	Thhalv10016128m	Phytozome 10
<i>Leavenworthia alabamica</i>	n.a. ¹	CoGe
<i>Neslia paniculata</i>	n.a. ¹	CoGe
<i>Schrenkiella parvula</i>	Tp4g22340	CoGe
<i>Sisymbrium irio</i>	n.a. ¹	CoGe
<i>Tarenaya hassleriana</i>	Th2v22033	CoGe

Angiosperm SPT5L homologs

<i>Amborella trichopoda</i>	evm_27.model.AmTr_v1.0_scaffold00002.356	Amborella Genome
<i>Arabidopsis lyrata</i>	487210	Phytozome 11
<i>Arabidopsis thaliana</i>	AT5G04290.1	TAIR
<i>Aquilegia coerulea</i>	Aquca_038_00139	Phytozome 11

<i>Boechera stricta</i>	Bostr.2128s0018.1.p	Phytozome 11
<i>Brachypodium distachyon</i>	Bradi2g20517.2.	Phytozome 11
<i>Brassica rapa</i>	Brara.J02756.1.p	Phytozome 11
<i>Capsella grandiflora</i>	Cagra.9217s0009 Org_	Phytozome 11
<i>Capsella rubella</i>	Carubv10000039m	Phytozome 11
<i>Citrus clementina</i>	Ciclev10030480m.g	Phytozome 11
<i>Citrus sinensis</i>	orange1.1g000247m	Phytozome 11
<i>Carica papaya</i>	evm.model.supercontig_188.8 evm.model.supercontig_53.150	Phytozome 11
<i>Eucalyptus grandis</i>	Eucgr.J01043.1	Phytozome 11
<i>Eutrema salsugineum</i>	Thhalv10015730m	Phytozome 11
<i>Fragaria vesca</i>	mrna23431.1-v1.0-hybrid	Phytozome 11
<i>Glycine max</i>	Glyma.10G276900.1 Glyma.20G112800.1	Phytozome 11
<i>Gossypium raimondii</i>	Gorai.011G234600.1	Phytozome 11
<i>Kalanchoe marnieriana</i>	Kalax.0009s0224.1.p	Phytozome 11
<i>Linum usitatissimum</i>	Lus10037946 Lus10038680	Phytozome 11
<i>Manihot esculenta</i>	Manes.07G094600.1.p	Phytozome 11
<i>Malus domestica</i>	MDP0000201216 MDP0000232228	Phytozome 11
<i>Medicago truncatula</i>	Medtr1g111560.1	Phytozome 11
<i>Mimulus guttatus</i>	Migut.F01946.1.p	Phytozome 11
<i>Oryza sativa</i>	LOC_Os05g43060.1	Phytozome 11
<i>Panicum hallii</i>	Pahal.C02415.1	Phytozome 11
<i>Panicum virgatum</i>	Pavir.Ca01318.1.p Pavir.Cb01635.1.p	Phytozome 11
<i>Phaseolus vulgaris</i>	Phvul.007G024600.1	Phytozome 11
<i>Populus trichocarpa</i>	Potri.008G032800.1 Potri.010G228800.1	Phytozome 11
<i>Ricinus communis</i>	29898.t000002	Phytozome 11
<i>Salix purpurea</i>	SapurV1A.0411s0080.1.p	Phytozome 11
<i>Theobroma cacao</i>	Thecc1EG043328t1	Phytozome 11
<i>Zea mays</i>	GRMZM2G370715_P01 GRMZM2G375222_P01	Phytozome 11

¹ Orthologs identified by similarity in unannotated genome. See methods for details.

² Short reads mapped to *Ar. lyrata* genomes for ortholog and SNP identification.

³ from Hollister, *et al.* (2012). Genetic adaptation associated with genome-doubling in autotetraploid *Arabidopsis arenosa*. *PLoS Genetics*, 8(12), e1003093.

Table S2: McDonald-Kreitman test of adaptive evolution.

	Polymorphic		Fixed		p-value
	Synon.	Nonsyn.	Synon.	Nonsyn.	
<i>Ar. thaliana</i> – <i>Ar. lyrata</i>					
Catalytic	58	59	71	51	n.s.
Ago platform	26	77	18	44	n.s.
<i>Ar. thaliana</i> – <i>Ar. arenosa</i>					
Catalytic	58	59	75	51	n.s.
Ago platform	26	77	24	48	n.s.
<i>Ar. thaliana</i> – <i>Bo. stricta</i>					
Catalytic	58	61	93	63	n.s.
Ago platform	26	80	39	59	n.s.
<i>Ar. thaliana</i> – <i>Cap. rubella</i>					
Catalytic	58	61	128	69	0.0481
Ago platform	26	77	42	64	n.s.
<i>Ar. thaliana</i> – <i>Ne. paniculata</i>					
Catalytic	59	59	104	65	n.s.
Ago platform	26	76	32	56	n.s.

n.s., not significant (FDR-adjusted $p < 0.05$)

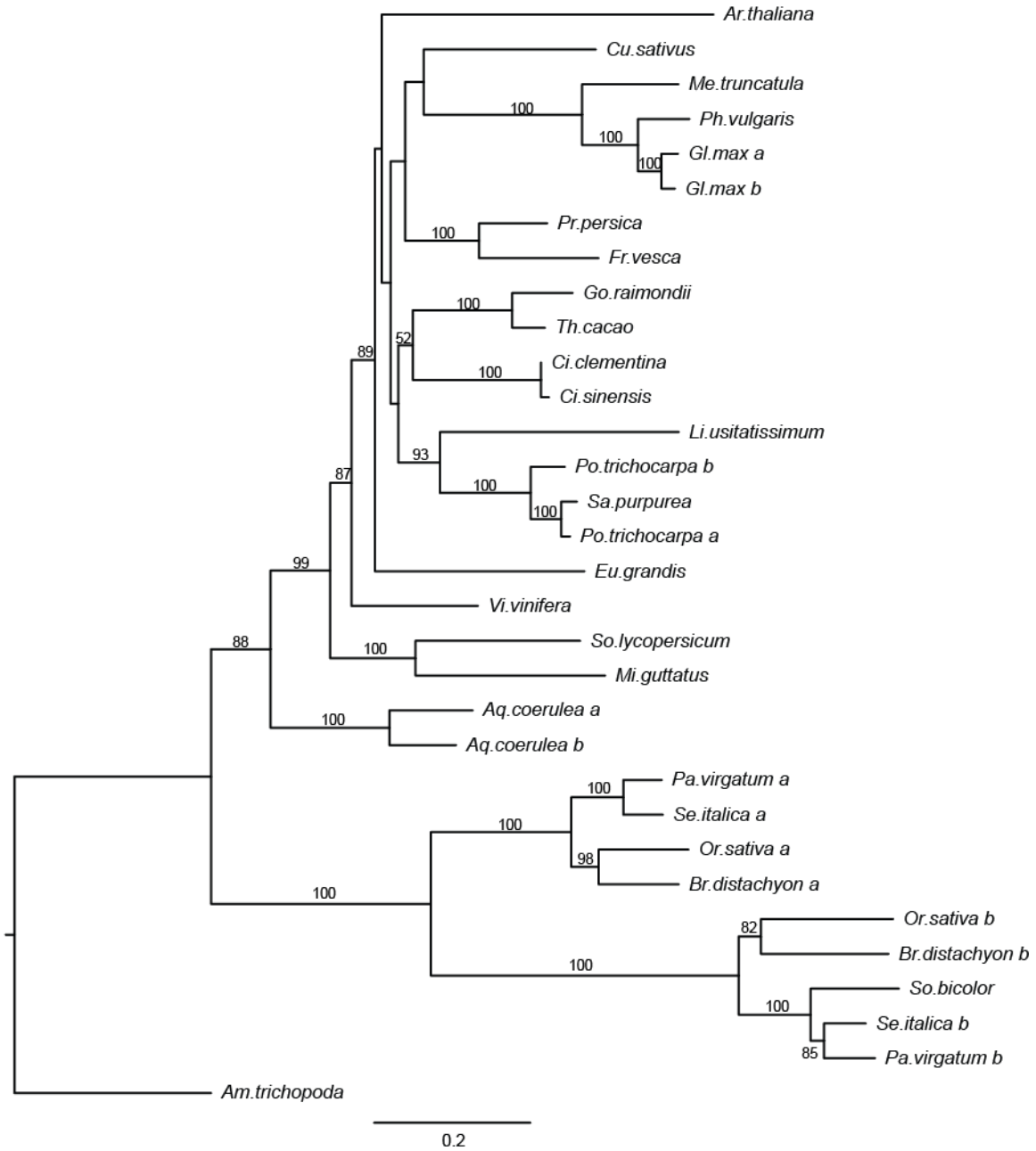


Figure S1. Phylogenetic relationship between NRPE1 orthologs analyzed in Figure 1. A maximum-likelihood tree generated from nucleotide sequence of catalytic domains A-H of 32 angiosperm NRPE1 orthologs. Positions in the alignment with a gap in >20% of taxa were removed. Branches list bootstrap support from 100 replicates when ≥ 50 . The gene tree conforms to accepted organismal phylogeny.

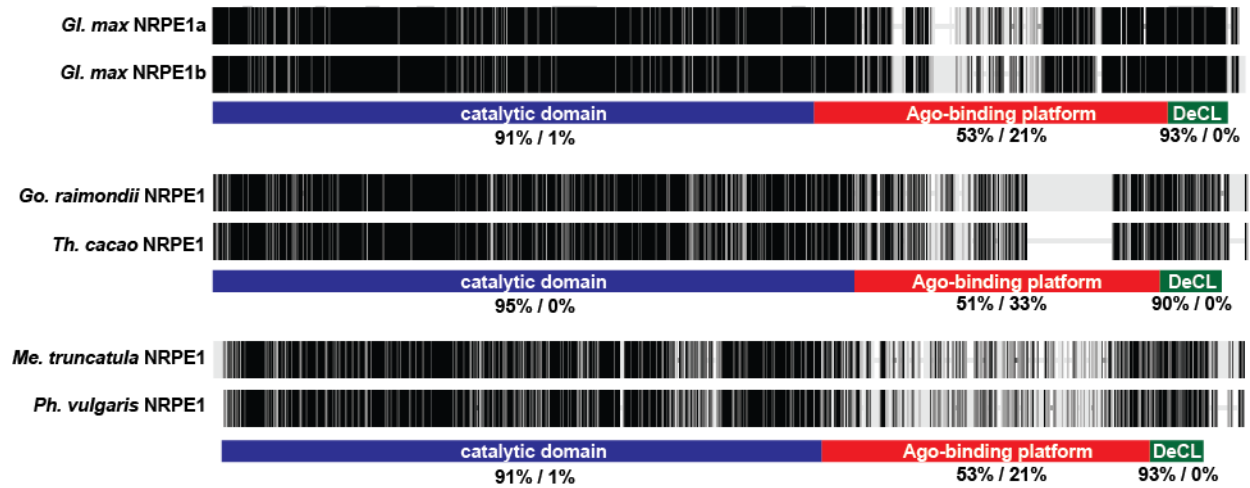


Figure S2. Pairwise comparison of NRPE1 orthologs. Amino acid sequences were aligned with MUSCLE. Identical positions are black and mismatches and gaps are gray. Values below the domain schematics are % positives / % gaps as measured with BLASTP.

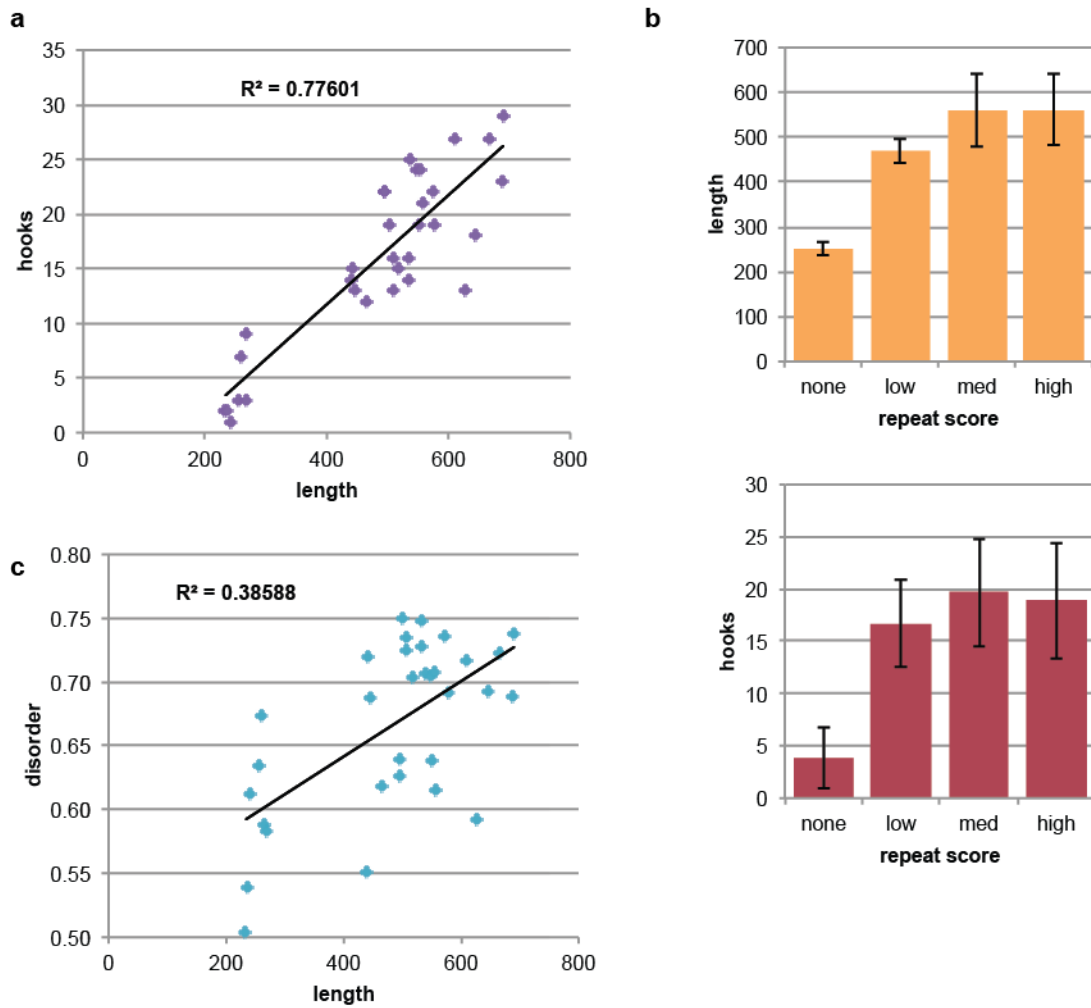


Figure S3. Conserved features of Ago-binding platforms are correlated. (a) Longer Ago-binding platforms have more Ago hooks. (b) Ago-binding platforms with higher repeat scores are longer (top) and have more Ago hooks (bottom). Error bars represent standard deviation of values in each group. Repeat score as listed in Table 1. (c) Longer Ago-binding platforms also have greater average disorder scores. Trend lines and R^2 values from a linear regression.

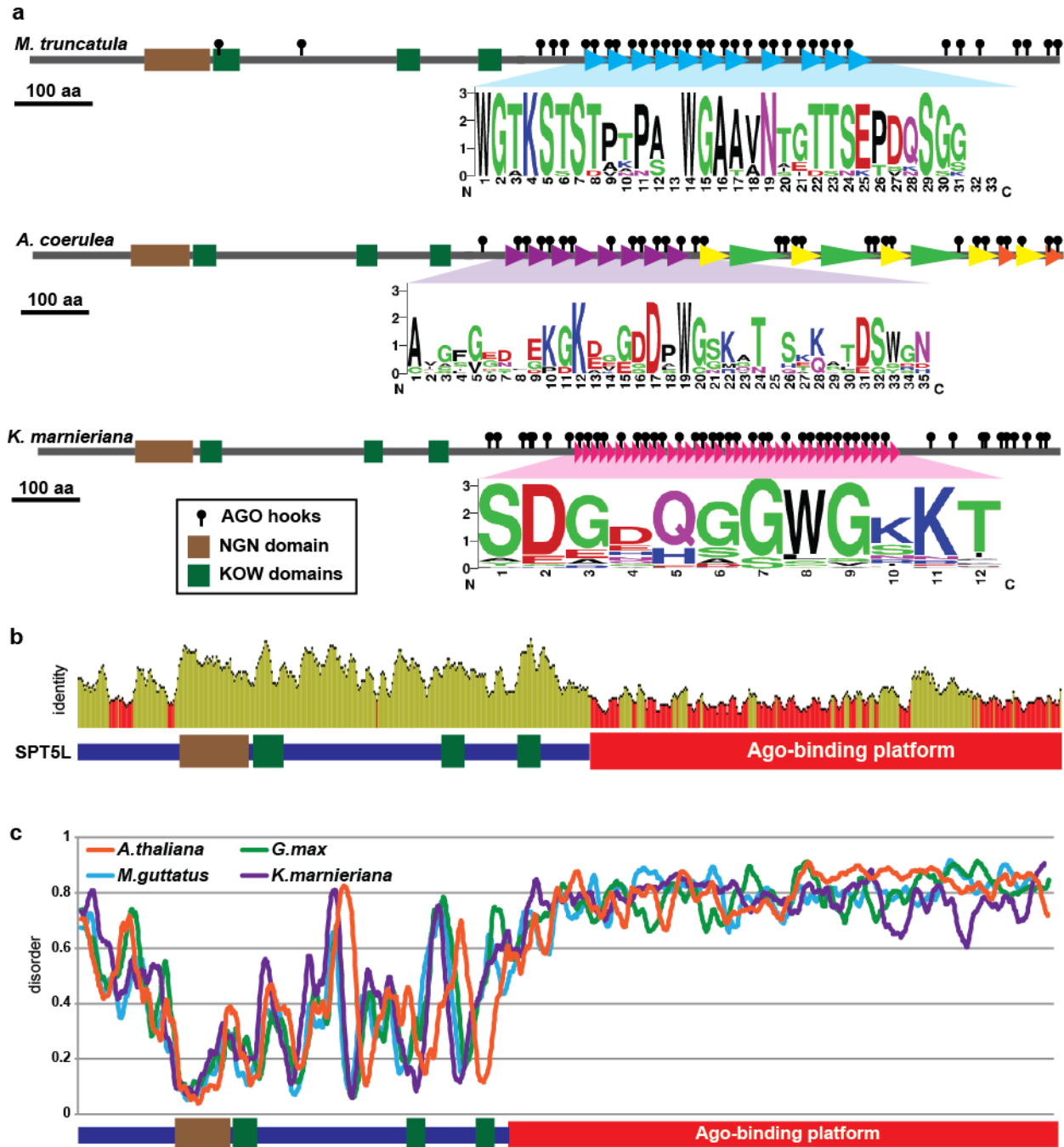


Figure S4. The Ago-binding platform of SPT5L is repetitive, non-conserved, and intrinsically disordered. (a) Representative SPT5L orthologs from across angiosperms demonstrate variation in the number, sequence, and conservation of tandem repeats in the Ago-binding platforms (colored triangles). (b) Identity between SPT5L orthologs from angiosperms is lowest in the C-terminal Ago-binding platform. After MUSCLE alignment columns with >20% gaps were stripped; a 10-amino acid sliding window of identity is displayed (above). The SPT5L domain structure is displayed below. (c) The Ago-binding platform is intrinsically disordered. IUPred disorder prediction for four SPT5L orthologs (*Arabidopsis thaliana*, *Glycine max*, *Mimulus guttatus*, *Kalanchoe marnieriana*); a 10-amino acid rolling average is plotted.

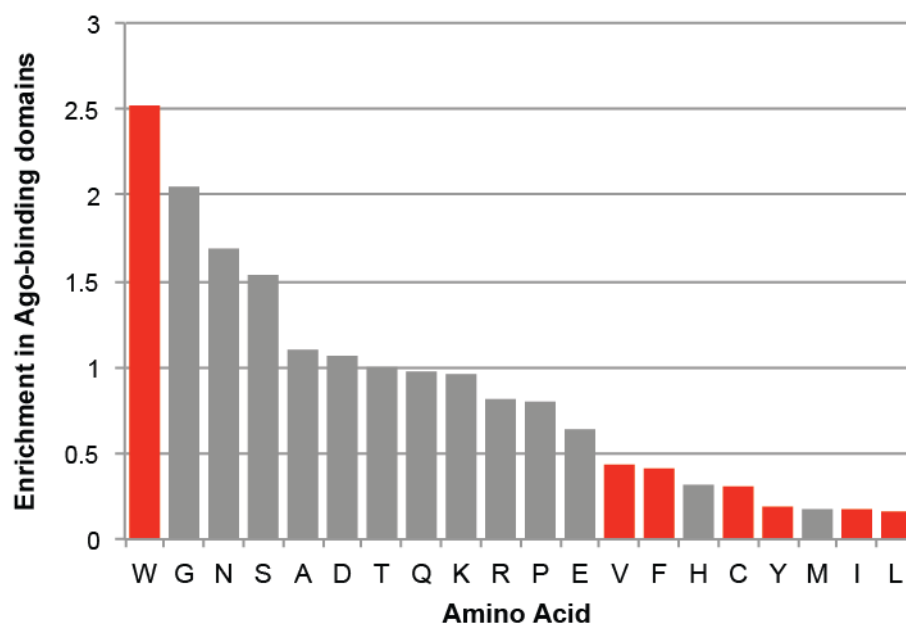


Figure S5. Depletion of order-promoting amino acids in Ago-binding platforms. Amino acids were arrayed by enrichment in Ago-binding platforms relative to other protein regions. Order-promoting amino acids are marked in red. Enrichment data from (Karlowski et al., 2010); order-promoting data from (Radivojac et al., 2007).

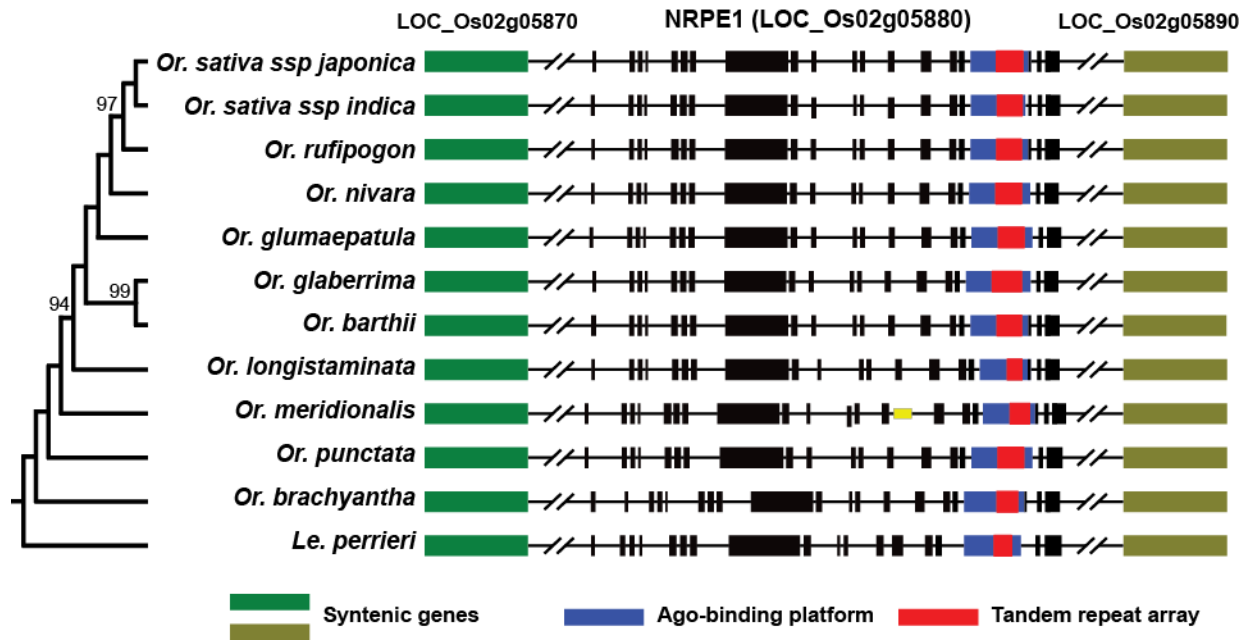


Figure S6. NRPE1a orthologs in the genus *Oryza*. Phylogenetic relationships between homologs are depicted on the left, based on a ML gene tree of the NRPE1a catalytic region. This gene tree recapitulates the expected species tree. Syntenic flanking genes are colored green and gold, with the *Or. sativa* gene identifier listed above. Boxes represent exons and lines represent introns. The Ago-binding platform is in blue, and the tandem repeats are in red. The small yellow box depicts missing sequence.

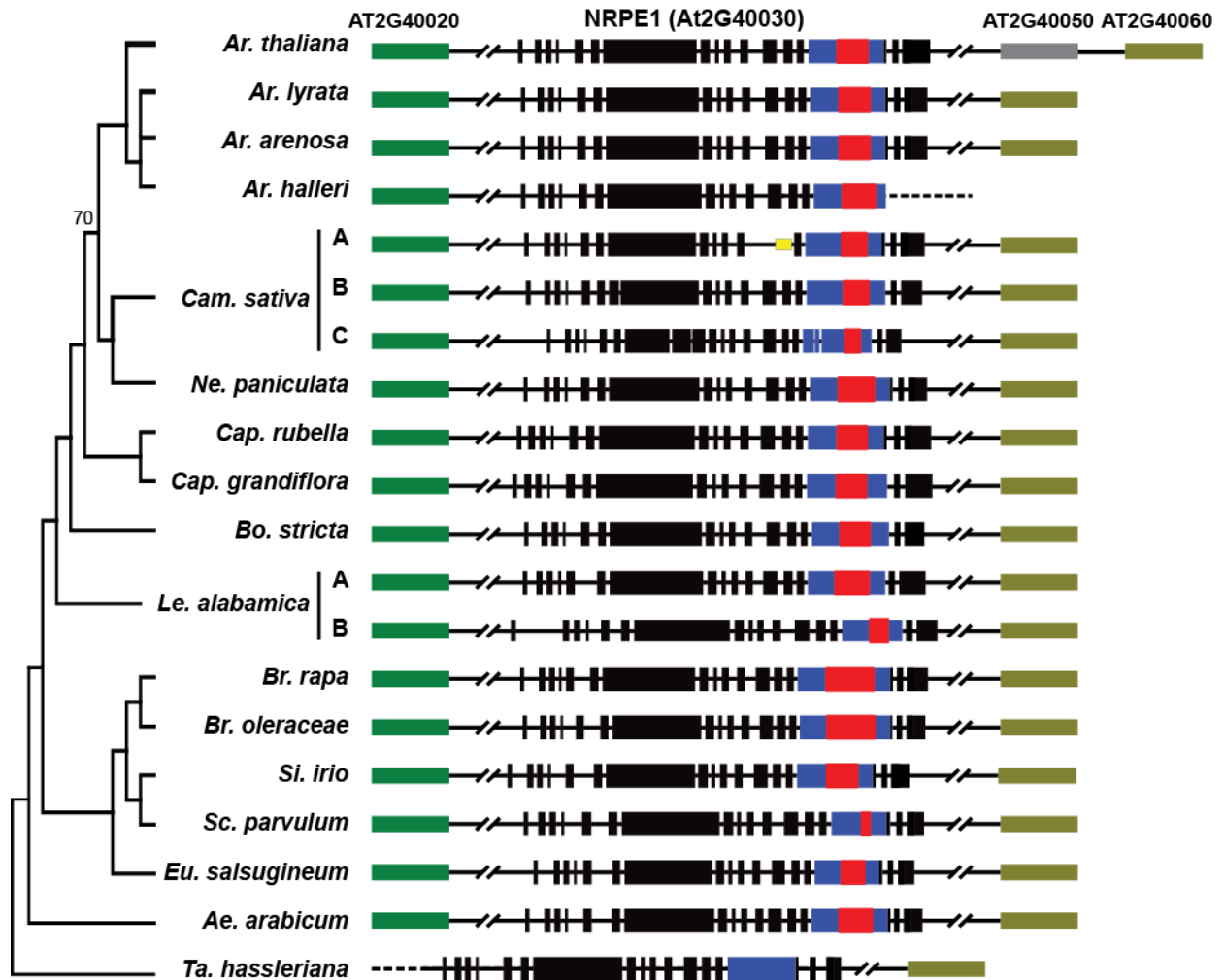


Figure S7. NRPE1 orthologs in the family Brassicaceae. Phylogenetic relationships between homologs are depicted on the left, based on a ML gene tree of the NRPE1 catalytic region. This gene tree recapitulates the expected species tree and includes recent polyploidization events in *Camelina sativa* and *Leavenworthia alabamica*. All features are colored as in Figure S7. The *T. hassleriana* sequence is at the end of a contig and does not have a left flanking gene.

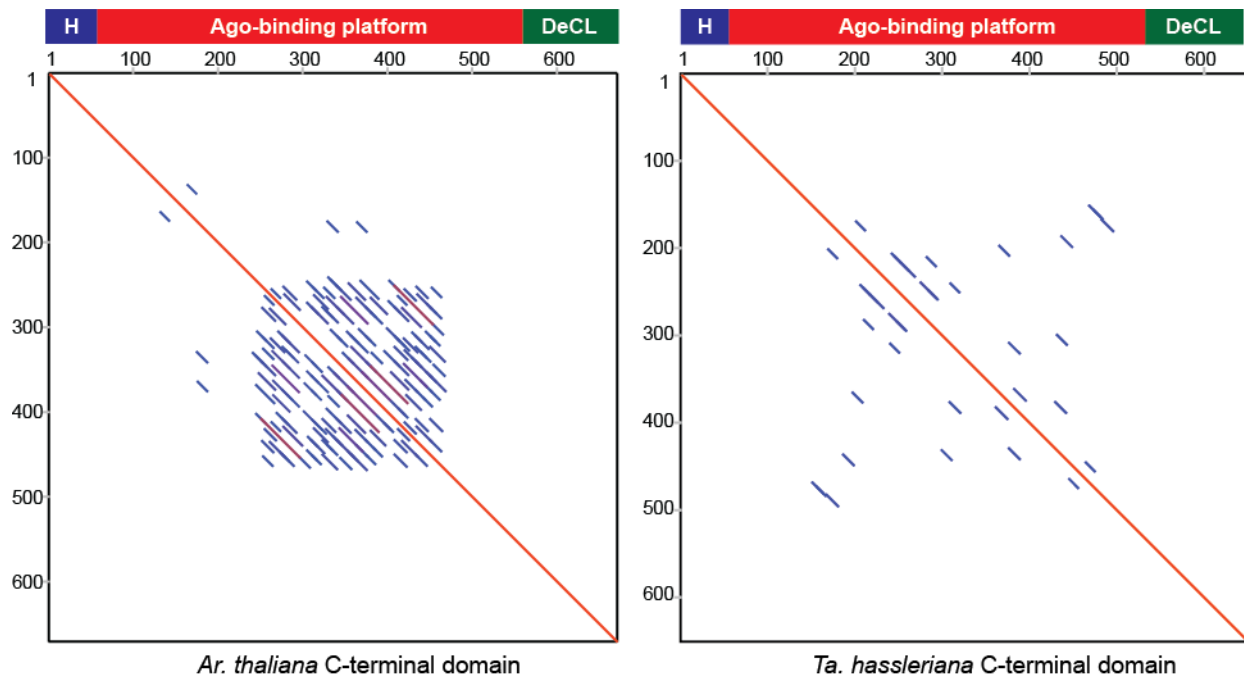


Figure S8. The *Ta. hassleriana* Ago-binding platform contains repetitive character. Self-alignment analysis (dot plots) demonstrates strong and weak repetitive character in *Ar. thaliana* (left) and *Ta. hassleriana* (right) carboxy terminal domains, respectively.

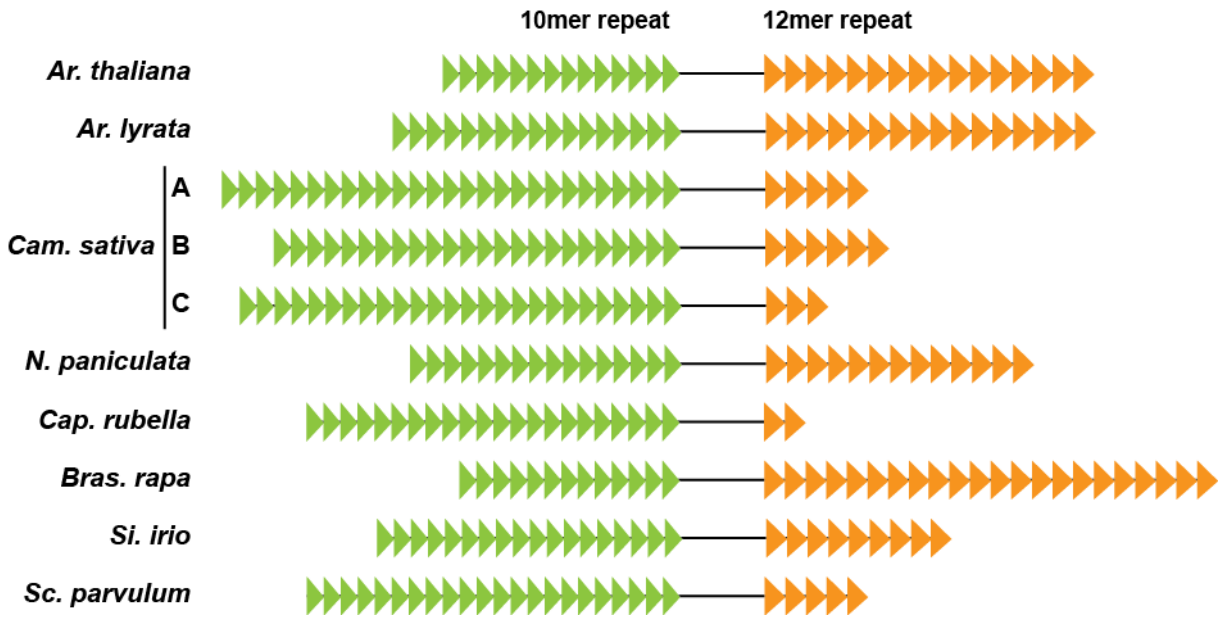


Figure S9. Variation in tandem repeats in the SPT5L Ago-binding platform. Diagram of tandem repeats from various Brassicaceae species, including three homeologs in *Camelina sativa* (A-C). All species have two distinct tandem repeat arrays found on separate exons and the sequence between the arrays is similar.

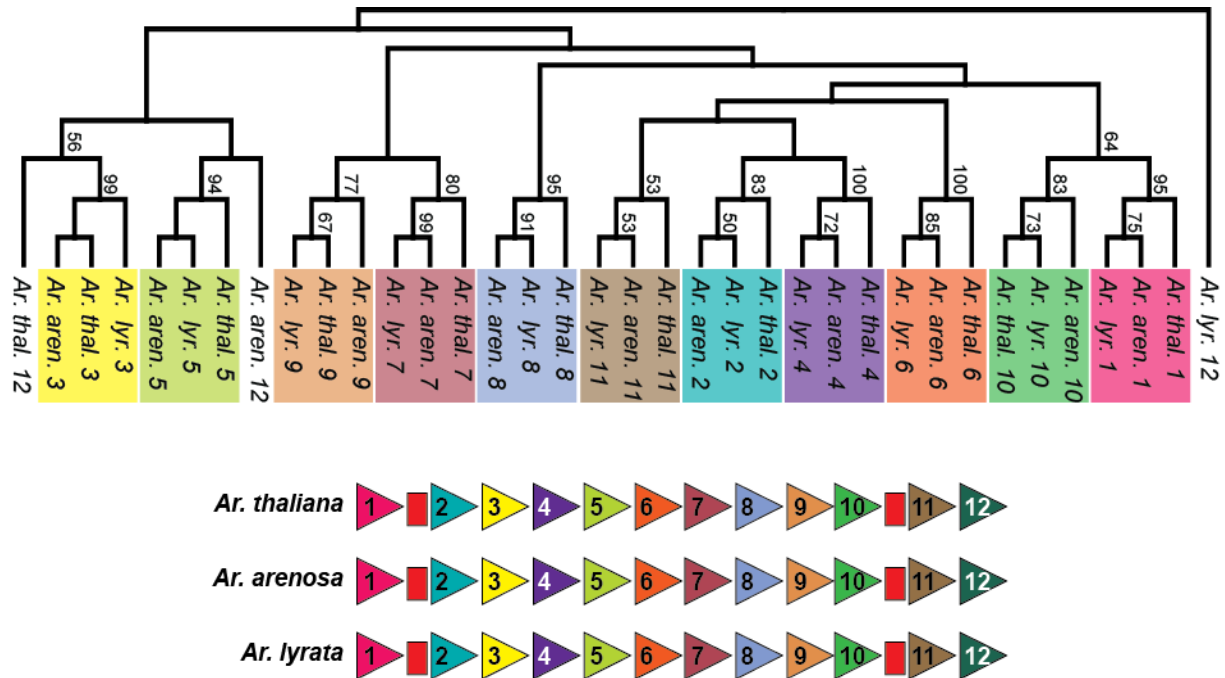


Figure S10. Phylogenetic analysis of repeats in the *Arabidopsis* genus demonstrates no changes in the NRPE1 repeat platform. (top) Cladogram based on ML tree of nucleotide sequence from individual repeats in *Ar. thaliana*, *Ar. arenosa*, and *Ar. lyrata* NRPE1 orthologs. Bootstrap values from 100 replicates are reported when ≥ 50 . (bottom) Diagram of tandem repeats in these species colored by phylogenetic relationships.

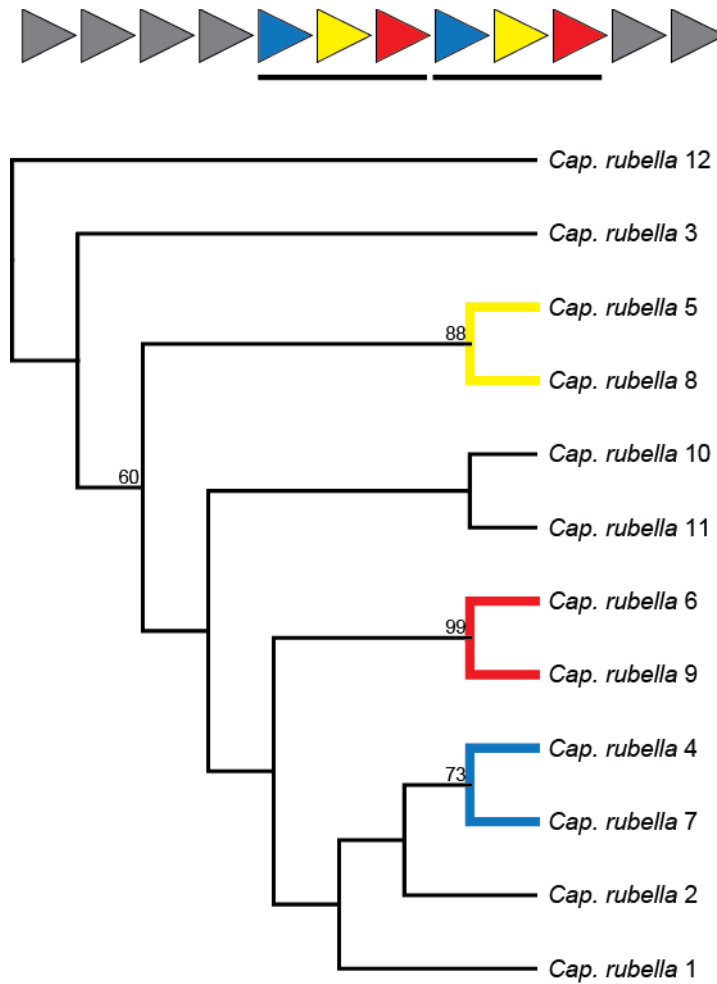


Figure S11. Phylogenetic analysis of *Capsella rubella* repeats supports a three-unit duplication. (top) Diagram of *Cap. rubella* tandem repeats colored by phylogenetic relationships. (bottom) Cladogram based on ML tree of individual repeats using nucleotide sequence. Bootstrap values from 100 replicates are reported when ≥ 50 .

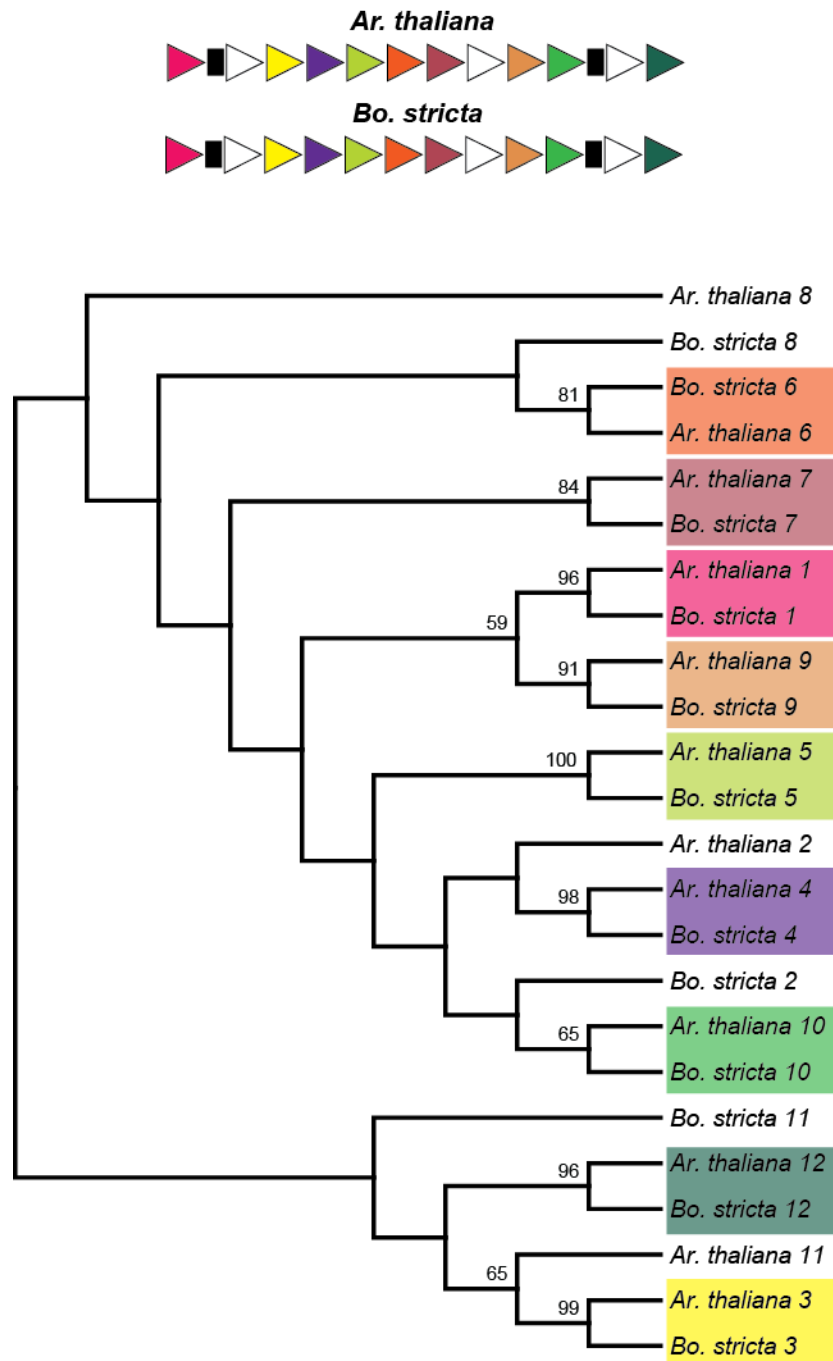


Figure S12. Phylogenetic analysis of *Boechera stricta* repeats demonstrates the ancestral repeat state. (top) Diagram of *Ar. thaliana* and *Bo. stricta* tandem repeat array showing identical placement of degenerate repeats. (bottom) Cladogram based on ML tree of individual *Ar. thaliana* and *Bo. stricta* repeat units shows colinearity of repeats. Bootstrap values from 100 replicates are reported when ≥ 50 .

SUPPORTING INFORMATION NOTES

Note S1. CDS sequences from angiosperm NRPE1 sequences listed in Table S1.

Note S2. CDS sequences from angiosperm SPT5L sequences listed in Table S1.

Note S3. CDS sequences from *Orzya* NRPE1 sequences listed in Table S1.

Note S4. CDS sequences from Brassicaceae NRPE1 sequences listed in Table S1.

All SI notes are .fasta files and can be opened with any text editor or DNA analysis software.

REFERENCES

Karlowski WM, Zielesinski A, Carrère J, Pontier D, Lagrange T, Cooke R. 2010. Genome-wide computational identification of WG/GW Argonaute-binding proteins in Arabidopsis. *Nucleic acids research* **38**: 4231–4245.

Radivojac P, Iakoucheva LM, Oldfield CJ, Obradovic Z, Uversky VN, Dunker AK. 2007. Intrinsic disorder and functional proteomics. *Biophysical Journal* **92**: 1439–1456.